

Molecular Mechanism for Regulation of the Human Mitochondrial Branched-Chain α -Ketoacid Dehydrogenase Complex by Phosphorylation

R. Max Wynn,^{1,2} Masato Kato,² Mischa Machius,¹ Jacinta L. Chuang,¹ Jun Li,¹ Diana R. Tomchick,¹ and David T. Chuang^{1,2,*}

¹Department of Biochemistry

²Department of Internal Medicine

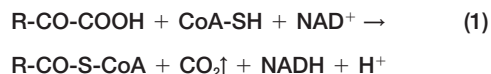
University of Texas Southwestern Medical Center
Dallas, Texas 75390

Summary

The human mitochondrial branched-chain α -ketoacid dehydrogenase complex (BCKDC) is a 4 MDa macromolecular machine comprising three catalytic components (E1b, E2b, and E3), a kinase, and a phosphatase. The BCKDC overall activity is tightly regulated by phosphorylation in response to hormonal and dietary stimuli. We report that phosphorylation of Ser292- α in the E1b active site channel results in an order-to-disorder transition of the conserved phosphorylation loop carrying the phosphoryl serine. The conformational change is triggered by steric clashes of the phosphoryl group with invariant His291- α that serves as an indispensable anchor for the phosphorylation loop through bound thiamin diphosphate. Phosphorylation of Ser292- α does not severely impede the E1b-dependent decarboxylation of α -ketoacids. However, the disordered loop conformation prevents phosphorylated E1b from binding the E2b lipoyl-bearing domain, which effectively shuts off the E1b-catalyzed reductive acylation reaction and therefore completely inactivates BCKDC. This mechanism provides a paradigm for regulation of mitochondrial α -ketoacid dehydrogenase complexes by phosphorylation.

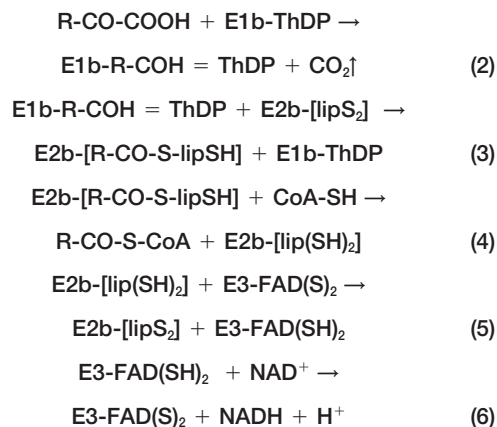
Introduction

The human branched-chain α -ketoacid dehydrogenase (BCKD) catalytic machine is a member of the highly conserved mitochondrial α -ketoacid dehydrogenase complexes comprising the BCKD complex (BCKDC), the pyruvate dehydrogenase complex (PDC), and the α -ketoglutarate dehydrogenase complex (Reed et al., 1985). The BCKDC catalyzes the oxidative decarboxylation of branched-chain α -ketoacids (BCKAs) derived from the branched-chain amino acids leucine, isoleucine, and valine (Chuang and Shih, 2001) (Reaction 1):



The 4×10^6 Da BCKDC is organized around a cubic core comprising 24 lipoyl-bearing dihydrolipoyl transacylase (E2b) subunits, with which multiple copies of branched-chain α -ketoacid decarboxylase/dehydrogenase (E1b), dihydrolipoamide dehydrogenase (E3), the BCKD kinase, and the BCKD phosphatase are associated. The

E1b and E2b components are specific for the BCKDC, whereas the E3 component is common among the three α -ketoacid dehydrogenase complexes (Reed et al., 1985). Reaction steps catalyzed by the three catalytic components (E1b, E2b, and E3) of BCKDC, which are linked through substrate channeling, are as follows:



The E1b component binds thiamin diphosphate (ThDP) and catalyzes the ThDP-mediated decarboxylation of α -ketoacids (Reaction 2), resulting in an enamine-ThDP intermediate (E1b-R-COH=ThDP), followed by the reductive transfer of the enamine to the lipoyl moiety covalently attached to E2b (abbreviated as E2b-[lipS₂]) (Reaction 3). The lipoyl-bearing domain (lip-LBD) carrying the S-acyldihydrolipoamide serves as a “swinging arm” (Perham, 2000) to transfer the acyl group from E1b to the E2b active site, where it is converted to acyl-CoA (Reaction 4). Finally, the E3 component with a tightly bound FAD moiety reoxidizes the dihydrolipoyl moiety on E2b (E2b-[lip(SH)₂]) (Reaction 5), with NAD⁺ as the ultimate electron acceptor (Reaction 6). The overall reaction results in the production of branched-chain acyl-CoA, CO₂, and NADH from BCKAs (Reaction 1).

The activities of BCKDC and PDC are regulated post-translationally by phosphorylation/dephosphorylation under various dietary conditions and hormonal stimuli (Reed et al., 1985; Harris et al., 1997). Rats fed low-protein diets show increased phosphorylation of the hepatic BCKDC (Harris et al., 1986). Starvation and diabetes stimulate activity of the BCKDC in skeletal muscle by decreasing the degree of phosphorylation of the enzyme complex (Paul and Adibi, 1982). The state of phosphorylation in the BCKDC was shown to largely correlate with the expression of the BCKD kinase in tissues, as regulated by extracellular stimuli (Zhao et al., 1993; Huang and Chuang, 1999). The BCKD phosphatase, which dephosphorylates the phosphorylated E1b, has been highly purified from bovine kidney (Damuni and Reed, 1987) but has not been cloned. The mechanism by which BCKD phosphatase regulates activity of the BCKDC is presently unknown.

Posttranslational modification of proteins by phosphorylation is a ubiquitous regulatory mechanism in

*Correspondence: david.chuang@utsouthwestern.edu

cells (Krebs et al., 1958). The human genome contains 575 protein kinase sequences representing 2% of the total genome (Lander et al., 2001). The structural basis for control by phosphorylation has been described (Johnson and Lewis, 2001). The size of the phosphoryl group on Ser73 of covalently modified phosphoducin causes the disordering of the N-terminal cap of helix 2, resulting in the inability of phosphoducin to bind $G_{\alpha\beta\gamma}$ subunits of heterotrimeric G proteins ($G_{\alpha\beta\gamma}$) in the activation/inactivation cycle (Gaudet et al., 1999). Phosphorylation on Ser14 of homodimeric glycogen phosphorylase induces conformational changes of the N-terminal residues, which results in a 50 Å shift of the serine residue so as to alter its contacts from those of intra- to intersubunit. This promotes a change in the orientation of the two subunits and the tertiary structure at the catalytic sites, leading to the activation of glycogen phosphorylase (Sprang et al., 1988). In contrast, the phosphorylation of Ser113 in *E. coli* isocitrate dehydrogenase does not produce conformational changes in the active site. Rather, inhibition is achieved by both charge and steric effects of the phosphoryl serine residue, and these effects block the access of the negatively charged isocitrate substrate to the active site (Hurley et al., 1990).

The regulation of the mammalian PDC by phosphorylation was first described as early as in the late 1960's (Linn et al., 1969). Despite this early discovery, the molecular mechanism underlying phosphorylation-induced inactivation of PDC and the cognate BCKDC by specific mitochondrial protein kinases remains unknown. In the human BCKDC, the two phosphorylation sites Ser292- α (site 1) and Ser302- α (site 2) (Cook et al., 1984) reside in a highly conserved phosphorylation loop in the E1b active site (Ævarsson et al., 2000; Fries et al., 2003; Li et al., 2004). Similarly, in the human PDC, the three phosphorylation sites are located in well-ordered loop regions, as shown in the 1.95 Å structure of its pyruvate dehydrogenase (E1p) component (Ciszak et al., 2003). It was proposed that a substitution of Ser264- α (phosphorylation site 1) with a glutamine in the E1p component mimics the phosphoryl group in partially inactivating the overall activity of the human PDC (Korotchkina and Patel, 2001). However, the structural basis for the inactivation of human E1p by the apparent size effect of the glutamine residue has not been deciphered.

In the present study, we use the E1b component of the human BCKDC as a model to dissect the molecular mechanism underlying the posttranslational control of mitochondrial α -ketoacid dehydrogenase complexes by phosphorylation. Our E1b crystal structures show that phosphorylation of Ser292- α results in an order-to-disorder transition of the loop conformation in the 15 Å long active site channel of phosphorylated E1b. This conformational change prevents the binding of lipoylated lipoyl-bearing domain (lip-LBD) to the E1b active site and effectively shuts off reductive acylation of lip-LBD (Reaction 3). By contrast, the ThDP-dependent decarboxylation of α -ketoacids (Reaction 2) is not severely impeded. These findings provide a framework for structure-based drug designs to intervene the phosphorylation-mediated regulation of α -ketoacid dehydrogenase complexes in disease states caused by the dysfunction

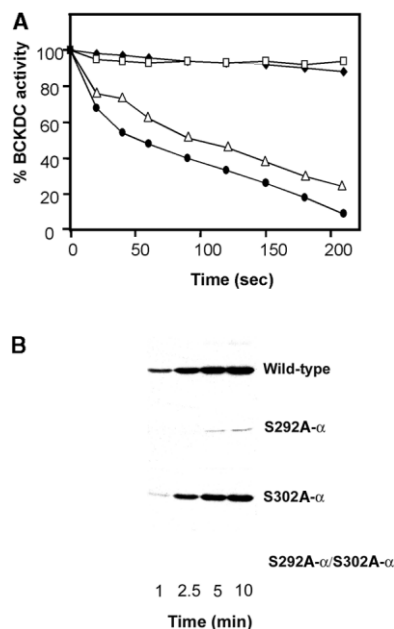


Figure 1. Time Course for Inhibition and Phosphoryl Group Incorporation of Wild-Type and Mutant BCKDC

(A) Inactivation of the overall activity of BCKDC. The phosphorylation of wild-type E1b (closed circles) and S292A- α (open squares), S302A- α (open triangles), as well as S292A- α /S302A- α (closed diamonds) mutant E1b (90 μ g each) was carried out in 0.1 ml volume in the presence of lipoylated E2b (144 μ g) and maltose binding protein-tagged rat BCKD kinase (26 μ g). The phosphorylation reaction was initiated with the addition of 2 mM $MgCl_2$ and 1 mM ATP. Aliquots (10 μ l) were taken at different times, and the activity of the reconstituted wild-type and mutant BCKDC was assayed.

(B) Kinetics for phosphoryl group incorporation into the E1b- α subunit. Phosphorylation of wild-type and mutant E1b proteins was conducted in 0.1 ml in the presence of lipoylated E2b (72 μ g) with wild-type or mutant E1b (45 μ g) and rat MBP-BCKD kinase (13 μ g). The phosphorylation reaction was initiated with the addition of 2 mM $MgCl_2$ and 0.4 mM [γ - ^{32}P]ATP (specific activity, 0.1 Ci/mmol). Aliquots (10 μ l) were taken at indicated times and subjected to SDS-PAGE. Radioactivity incorporated into the E1b- α subunit was scanned by storage phosphorimaging.

of these mitochondrial catalytic machines. These include heritable Maple Syrup Urine Disease (Chuang and Shih, 2001), primary lactic acidosis (Robinson, 2001), and type II diabetes (Majer et al., 1998).

Results and Discussion

Residue Ser292- α Is the Major Phosphorylation Site

Phosphorylation of wild-type E1b and a site 2 E1b mutant (S302A- α), in which only site 1 is phosphorylated, results in a near complete rapid inactivation of the reconstituted BCKDC (Reaction 1) in 3.5 min (Figure 1A). In contrast, phosphorylation of site 2 in the S292A- α variant, in which site 1 is abolished, is without effect on the reconstituted BCKDC activity over the same time period. The S292A- α /S302A- α mutant, in which both phosphorylation sites are abolished, also remains fully active over the entire incubation period. The time course for incor-

Table 1. Kinetic Parameters for the Decarboxylation Reaction Catalyzed by Wild-Type and Phosphorylated and Mutant E1b Proteins

E1b Protein	K_m (KIV) (μM) ^a	k_{cat} (min^{-1})	k_{cat}/K_m ($\text{min}^{-1} \mu\text{M}^{-1}$) ($\times 10^2$)
Wild-type	50 \pm 3	12 \pm 0.3	24
S302A- α	22 \pm 4	37 \pm 2	170
S292- α -PO ₃	983 \pm 10	9 \pm 1	0.9
S292D- α	4,896 \pm 88	99 \pm 7	2.0
S292E- α	593 \pm 18	7.7 \pm 0.5	1.3
S292N- α	224 \pm 14	166 \pm 12	74
S292Q- α		0	

Phosphorylation and mutational studies on Ser292- α (site 1) were carried out with the S302A- α mutant, in which phosphorylation site 2 is abolished. For simplicity, the S302A- α substitution is not indicated in the nomenclature.

^aKIV, α -ketoisovalerate.

poration of the [³²P] phosphoryl group from [γ -³²P]ATP into the two phosphorylation sites was also investigated. The rate and degree of [³²P] incorporation into wild-type E1b is in parallel to that of the S302A- α (site 2) mutant (Figure 1B). Only a trace amount of the [³²P] label is incorporated into site 2 of the S302A- α variant in the same time frame. We have previously shown that E1b activity is completely abolished at the end of an 8 min incubation. Abolition of activity at this time point corresponded to 50% of the maximal [³²P] incorporation (Davie et al., 1995), and the endpoint for incorporation was achieved in 2 hr (data not shown). This finding is consistent with the pioneer study by Sugden and Randle (1978), which reported that the phosphorylation of only one of the two α chains in the E1p heterotetramer is sufficient to inhibit both E1p active sites.

The above results confirm that the phosphorylation of Ser292- α alone is sufficient and necessary to inactivate the BCKDC, and that Ser302- α is a silent phosphorylation site (Zhao et al., 1994). In the cognate E1p component of the bovine PDC, phosphorylation proceeds markedly faster at site 1 than at sites 2 and 3, and phosphorylation at site 1 also correlates closely with the inactivation of PDC (Yeaman et al., 1978). Therefore, the remaining studies focus on the mechanism by which phosphorylation on Ser292- α inactivates the BCKDC. To ensure that both of its active sites were phosphorylated, the S302A- α E1b mutant was incubated with Mg-ATP, lipoylated E2b (lip-E2b), and the MBP kinase for 8 hr and was used in kinetic and crystallographic studies.

Phosphorylation on Ser292- α Increases

K_m without Significantly Affecting k_{cat} of E1b-Catalyzed Decarboxylation (Reaction 2)

The E1b-catalyzed decarboxylation (Reaction 2), which is distinct from the overall activity of the BCKDC (Reaction 1), was assayed in the presence of an artificial electron acceptor, 2,6-dichlorophenolindophenol (DCPIP). Table 1 shows that K_m for substrate α -ketoisovalerate (KIV) and k_{cat} (based on the E1b heterotetramer) of the S302A- α mutant are similar to those of the wild-type. Therefore, phosphorylation and mutational studies on site 1 were carried out with the S302A- α substitution present in all variants. For simplicity, the S302A- α substitution is not included in the nomenclature of these mutants.

Phosphorylation at site 1 alone with the S302A- α mu-

tant, designated as S292- α -PO₃ E1b, results in a \sim 20-fold increase in K_m for KIV, with a 25% decrease in k_{cat} compared to the wild-type (Table 1). The S292D- α mutant shows a marked \sim 100-fold higher K_m for KIV and an 8-fold higher k_{cat} than the wild-type. The S292E- α mutant shows a 12-fold increase in K_m for KIV and a small decrease in k_{cat} from the wild-type. An uncharged residue, such as asparagine or glutamine, was also introduced into site 1 to determine the effects of residue size on E1b-catalyzed decarboxylation. The S292N- α mutant exhibits a 4-fold higher K_m for KIV and a 14-fold higher k_{cat} than the wild-type. Remarkably, the presence of a bulky uncharged glutamine residue alone in the S292Q- α substitution is sufficient to completely eliminate E1b-catalyzed decarboxylation (Table 1).

Using the same assay, we showed previously that substitutions of invariant residues that form a hydrogen bond network in the conserved phosphorylation loop also result in marked increases in k_{cat} for E1b-catalyzed decarboxylation for these mutants (Li et al., 2004). The elevated rates of E1b-catalyzed decarboxylation measured by DCPIP reduction with the mutants are identical to those determined radiochemically by monitoring ¹⁴CO₂ evolution by using [1-¹⁴C]KIV as a substrate in the presence of DCPIP. The Perham group has previously reported similar results regarding an increased rate of decarboxylation with a reduced activity for reductive acetylation resulting from limited proteolysis or amino acid substitutions in the corresponding loop region of E1p from *Bacillus stearothermophilus* (Chauhan et al., 2000; Fries et al., 2003).

Phosphorylation on Ser292- α Nullifies the Overall Activity of BCKDC

The BCKDC was reconstituted with wild-type or phosphorylated or mutant E1b in the presence of stoichiometric amounts of lip-E2b and E3. The K_m for KIV and k_{cat} of the BCKDC overall activity (Reaction 1) reconstituted with the S302A- α single mutant are similar to the wild-type (Table 2). Despite significant E1b-catalyzed decarboxylation activity (Table 1), phosphorylation of Ser292- α (S292- α -PO₃) in the S302A- α mutant completely abolishes its overall activity (Reaction 1) (Table 2). The S292D- α substitution produces a reduced (to 18%) k_{cat} and an over 90-fold higher K_m for KIV of the reconstituted overall activity relative to the wild-type BCKDC, whereas the BCKDC activity reconstituted with the S292E- α mu-

Table 2. Kinetic Parameters for the Overall Reaction Catalyzed by the BCKD Complex Reconstituted with Wild-Type, Phosphorylated, and Mutant E1b

E1b Protein	K_m (KIV) (μM) ^a	k_{cat} (min^{-1})	k_{cat}/K_m ($\text{min}^{-1} \mu\text{M}^{-1}$)
Wild-type	48 ± 2	198 ± 9	4
S302A- α	28 ± 3	131 ± 8	4.6
S292- α -PO ₃		0	
S292D- α	4,381 ± 85	35 ± 3	0.0079
S292E- α		0	
S292N- α	193 ± 14	235 ± 10	1.21
S292Q- α		0	

Phosphorylation and mutational studies on Ser292- α (site 1) were carried out with the S302A- α mutant, in which phosphorylation site 2 is abolished. For simplicity, the S302A- α substitution is not indicated in the nomenclature.

^aKIV, α -ketoisovalerate.

tant is abolished. The S292N- α variant shows a 4-fold higher K_m for KIV and an \sim 20% higher k_{cat} of the reconstituted overall activity than the wild-type. The presence of the bulky uncharged glutamine residue in the S292Q- α mutant nullifies the overall activity (Table 2), similar to phosphorylated and S292E- α E1b (Table 1). The above results show that while E1b-catalyzed decarboxylation is apparently affected by phosphorylation or substitutions at Ser292- α , the altered k_{cat} values for this reaction (Table 1) do not necessarily correlate with k_{cat} values for the overall activity of the BCKDC reconstituted with these phosphorylated or mutant E1b proteins.

The Presence of a Phosphoryl Group on Ser292- α Interferes with ThDP Binding

Binding measurements were based on fluorescence quenching upon the binding of increasing concentrations of ThDP to E1b (Nemeria et al., 2001). The fluorescence quenching was corrected for inner filter effects at high ThDP concentrations. The fluorescence quenching measurements allow direct determinations of the dissociation constant (K_d) for ThDP binding to wild-type and mutant E1b, including variants that do not exhibit activity for E1b-catalyzed decarboxylation (Reaction 2). As shown in Table 3, phosphorylation of Ser292- α in the S302A- α mutant results in a 55-fold higher dissociation constant than the wild-type. The replacement of Ser292- α with a charged or an uncharged residue invariably increases the dissociation constant by one order of magnitude. The above results are consistent with 5- to 14-fold increases in K_m for ThDP for the E1b site 1 mutants that exhibit activity for the reconstituted BCKDC (data not shown). The C2 carbon of ThDP and the putative substrate binding site (near His146- β') (Ævarsson et al., 1999) are within 2–3 Å of each other (Wynn et al., 2003).

Table 3. Dissociation Constants (K_d) for the Binding of ThDP to E1b Proteins as Determined by Fluorescence Quenching

	K_d (μM)	Maximum Quench (%)
Wild-type	1.6 ± 0.1	57.0 ± 5.7
S292- α -PO ₃	89.3 ± 5.8	62.4 ± 0.4
S292D- α	40.3 ± 3.2	74.6 ± 2.0
S292E- α	52.6 ± 1.7	73.1 ± 2.2
S292N- α	54.4 ± 7.1	78.4 ± 2.3
S292Q- α	60.9 ± 7.0	76.5 ± 4.5

Thus, the reduced affinity of ThDP may explain, in part, the significantly higher than wild-type K_m for KIV displayed by these phosphorylated and mutant E1b proteins.

Phosphorylation of Ser292- α Eliminates E1b-Catalyzed Reductive Acylation

The reductive acylation reaction (Reaction 3) catalyzed by E1b was assayed by using [U-¹⁴C]KIV and lip-LBD as substrates, and the rate of radiolabel incorporation into the latter substrate was determined. This assay is based on a combination of Reactions 2 and 3, and this combination allows the measurement of the latter reaction, since the former is irreversible and not rate limiting. The phosphorylation of Ser292- α in the S302A- α mutant abolishes the reductive acylation activity of this variant (Figure 2). A residual or absent reductive acylation activity is also exhibited by the S292Q- α and S292E- α mutants. A markedly lower (11%) than wild-type level of reductive acylation activity is present in the S292D- α

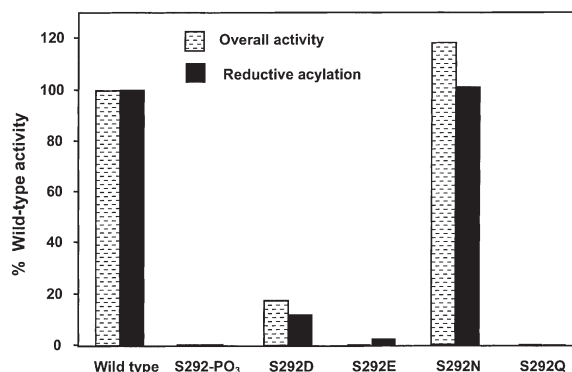


Figure 2. Activity Levels for the Reconstituted Overall Reaction and Reductive Acylation of Wild-Type, Phosphorylated, and Mutant E1b Proteins

The overall activity of the reconstituted BCKDC and the reductive acylation of lip-LBD catalyzed by wild-type or mutant E1b was assayed as described in the Experimental Procedures. Activity for reductive acylation is expressed as a percent relative to the wild-type (2.3 min^{-1}). Results are the averages of two independent experiments. The overall BCKDC activity is expressed as percent k_{cat} of the reconstituted wild-type BCKDC (198 ± 9 min^{-1}) from Table 2.

mutant. In contrast, the S292N- α variant shows the wild-type level of reductive acylation activity.

The residual or absent reductive acylation activities obtained with phosphorylated and mutant E1b show close parallels to reductions in k_{cat} values of the BCKDC overall activity reconstituted with these E1b proteins (Figure 2). The data support the thesis that the reductive acylation step (Reaction 3) is rate limiting in the overall reaction (Reaction 1) catalyzed by the BCKDC (Li et al., 2004, Fries et al., 2003). More significantly, the results indicate that phosphorylation of Ser292- α inactivates the BCKDC by abolishing the E1b-catalyzed reductive acylation reaction.

The Phosphoryl Group on Ser292- α Prevents E1b from Binding Lip-LBD

To provide a biochemical basis for the decreased level or absence of reductive acylation activity in phosphorylated or mutant E1b, isothermal titration calorimetry (ITC) was employed to measure the binding of lip-LBD to E1b. A typical thermogram (upper panel) and the binding isotherm (lower panel) for the interactions of lip-LBD with wild-type E1b show a binding molar ratio of E1b heterotetramer:lip-LBD monomer of 1:2 (Figure 3). No heat changes are produced when lip-LBD is titrated against phosphorylated E1b (S292- α -PO₃), indicating the absence of binding. The curve-fitting analysis of the binding isotherm shows a dissociation constant (K_d) of 1.8×10^{-5} M for the binding of lip-LBD to wild-type E1b. The S292N- α mutant, which shows a wild-type k_{cat} value for the overall reaction (Table 2), also binds lip-LBD with a dissociation constant ($K_d = 2.8 \times 10^{-5}$ M) similar to the wild-type. The S292D- α variant exhibits residual reconstituted BCKDC activity; however, the binding of lip-LBD to this mutant E1b is too weak to be detected by ITC. The S292E- α and S292Q- α mutants, which do not show reconstituted BCKDC activity, also do not produce heat changes ($\Delta H^\circ = 0$) when titrated with lip-LBD, indicating the inability of these mutant E1bs to bind lip-LBD, similar to phosphorylated E1b. Since lip-LBD is a substrate for Reaction 3, the void in interactions between this domain and phosphorylated, as well as S292E- α and S292Q- α mutant E1b, explains the absence of reductive acylation activity with these E1b proteins. The abrogation of reductive acylation activity resulting from the failure of mutant E1b to bind lip-LBD was also observed with the H291A- α (Wynn et al., 2003) and the phosphorylation loop E1b mutants (Li et al., 2004).

Phosphorylation of Ser292- α (Site 1) Induces Order-to-Disorder Transition of the Phosphorylation Loop

To provide a structural basis for the inactivation of the BCKDC by phosphorylation, crystal structures of wild-type, phosphorylated and mutant human E1b proteins were determined by X-ray crystallography. We found that N-terminally His₆-tagged E1b proteins gave higher quality crystals when in complex with the subunit binding domain (SBD) of the human E2b component. These crystals are overall similar to those described previously for free wild-type E1b protein (Wynn et al., 2003; Li et

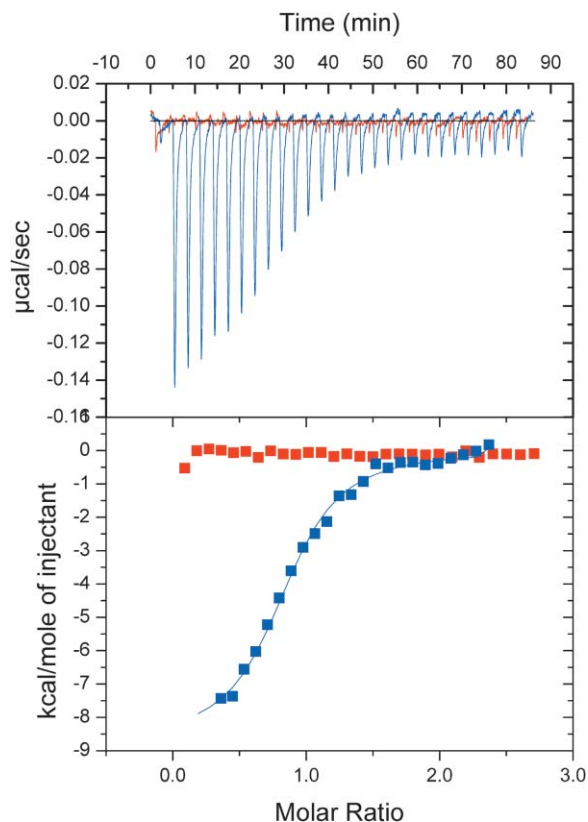


Figure 3. The Binding of lip-LBD to Wild-Type and Phosphorylated E1b Measured by Isothermal Titration Calorimetry

Wild-type (in blue) or phosphorylated (in red) E1b protein (75 μ M) was titrated with 1.5 mM lip-LBD (residues 1–84) as described in the Experimental Procedures. The upper panel represents raw isotherm data with time obtained over a series of 28 injections with wild-type or phosphorylated E1b. The lower panel shows the binding isotherms plotted against the molar ratio of E1b heterotetramer:lip-LBD. The data were fit by using ORIGIN v. 7.0 software. For wild-type E1b, the dissociation constant K_d is 2.62×10^{-5} M; for phosphorylated E1b, there is no detectable binding.

al., 2004). The active site structure of wild-type E1b determined at 1.83 Å resolution from the E1b-SBD complex is indistinguishable from that of free C-terminally His₆-tagged wild-type E1b determined previously (Wynn et al., 2003). SBD binds to the C termini of the two β subunits in the E1b heterotetramer. It crosses the 2-fold crystallographic axis that coincides with the intrinsic 2-fold E1b $\alpha|\beta'$ dimer axis. The corresponding electron density is therefore overlapped and averaged and does not allow unambiguous modeling of the SBD portion.

Figure 4A shows the segment corresponding to Arg287- α to Arg301- α of the conserved phosphorylation loop region (residues 286–314) in one of the two identical active site channels for wild-type E1b in the absence of substrate, which harbors cofactor ThDP. This segment contains Ser292- α (phosphorylation site 1) and a small C-terminal helix with the electron density interrupted between Ser302- α (phosphorylation site 2) and Asp305- α . The phosphorylation loop as shown covers 1072 Å² of the surface area and consti-

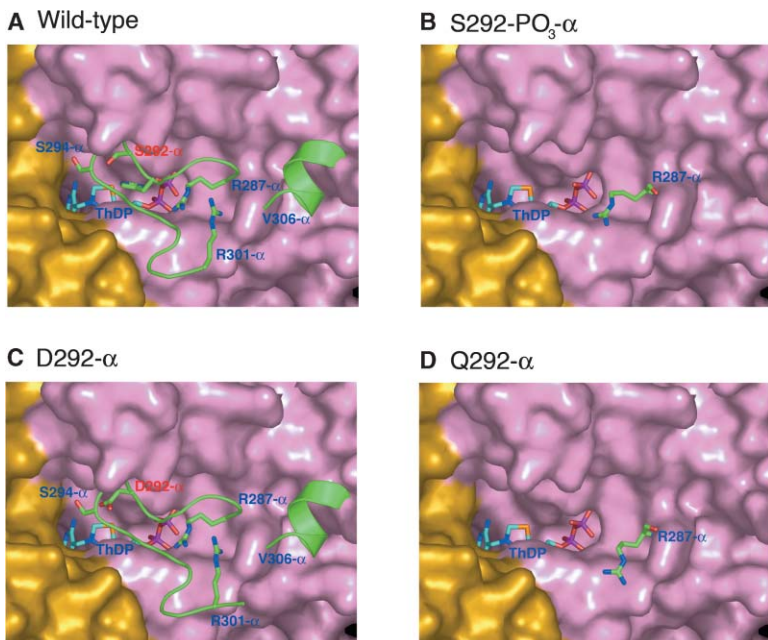


Figure 4. The Phosphorylation Loop and Bound ThDP against the Surface Contour of the E1b Active Site Channel Formed by the α (purple) and the β' (bronze) Subunits

(A) The wild-type phosphorylation loop (in green) from the α subunit as viewed down the 15 Å long active site channel. Ser292- α (phosphorylation site 1) is labeled in red. (B) The wild-type E1b was phosphorylated in the absence of ThDP and substrate. Crystals of the phosphorylated E1b-SBD complex were soaked in the crystallization buffer containing 10 mM Mn-ThDP. The phosphorylation loop in S292- α -PO₃ E1b is largely disordered, and R287- α is only partially ordered. (C) The loop in the S292D- α mutant is also ordered, in part, through interactions between Asp292- α and Ser294- α . (D) The loop in the S292Q- α variant is also disordered, similar to the S292- α -PO₃ structure.

tutes part of the inner wall for the 15 Å deep active site channel. The C2 carbon in the thiazolium ring of cofactor ThDP is at the bottom of the active site channel. The side chain of Ser292- α is buried inside in the ordered loop conformation.

The wild-type E1b was phosphorylated in the absence of ThDP and substrate. Crystals of the phosphorylated E1b-SBD complex were then soaked in a buffer containing 10 mM Mn-ThDP. Figure 4B shows that phosphorylation of Ser292- α results in a complete absence of electron density for the loop, except for Arg287- α and Tyr286- α , which adopts a different conformation compared to the wild-type (the latter residue was not shown in the figure). Since fully phosphorylated E1b is used in crystallographic studies, the missing electron density for the loop reflects a disordered conformation in the two identical active sites. Thus, the structural data obtained here in the absence of substrate do not shed light on the flip-flop mechanism between the two active sites proposed for other ThDP-dependent enzymes (Ciszak et al., 2003; Lu et al., 2000). A substitution of Ser292- α with a small negatively charged aspartic acid residue maintains an ordered but altered (see below) loop conformation (Figure 4C). The replacement of Ser292- α with a large neutral glutamine residue also induces an order-to-disorder transition of the phosphorylation loop (Figure 4D) analogous to that observed in phosphorylated E1b. There is also no electron density for the phosphorylation loop when Ser292- α is changed to an asparagine or glutamate residue (data not shown).

The binding site for lip-LBD in the E1b active site channel is unknown. Nonetheless, except for the S292N- α mutant, a good correlation exists between the crystallographically characterized disordering of the phosphorylation loop and the inability of E1b to bind lip-LBD (Wynn et al., 2003; Li et al., 2004). We interpret the results to indicate that the ordered phosphorylation loop directly or indirectly provides the determinants for lip-LBD rec-

ognition in the E1b active site. This is invariant with many examples of loops that only become ordered upon ligand binding. These include the ATP-lid conformations in branched-chain α -ketoacid dehydrogenase kinase (Machius et al., 2001) and the histidine-protein kinase CheA (Bilwes et al., 2001), with both conformations promoted by ATP binding, as well as the ordered phosphorylation loop in the E1b active site induced by bound ThDP (Li et al., 2004; Nakai et al., 2004). The wild-type binding affinity of the S292N- α mutant for lip-LBD suggests a local disruption of the phosphorylation loop that renders the loop partially flexible, but not to the extent of an overall disruption that abolishes the determinants for lip-LBD recognition. The local disruption of the phosphorylation loop in the S292N- α mutant corresponds to its markedly reduced affinity for ThDP binding (Table 3).

The k_{cat} for E1b-catalyzed decarboxylation is markedly higher than the wild-type in certain variant E1b proteins, in which the phosphorylation loop conformation is either ordered (S292D- α) or locally displaced and showing increased flexibility (S292N- α). The results indicate that, unlike reductive acylation (Reaction 3), a completely ordered phosphorylation loop is not required for E1b-catalyzed decarboxylation (Reaction 2). However, a local displacement or an overall disruption of the phosphorylation loop could in turn also change the rate of enamine-ThDP turnover, resulting in a markedly altered k_{cat} or a complete absence (S292Q- α) of E1b-catalyzed decarboxylation activity.

Introduction of Negative Charges Alone Does Not Disrupt the Loop Conformation

Figure 5A shows the phosphorylation loop (Arg287- α to Arg301- α) conformation that, when combined with the hydrophobic pocket provided by the β' subunit, forms the active site channel of wild-type human E1b. The α -ketoacid substrate, as indicated by an arrow here, must travel the entire length of the 15 Å active site

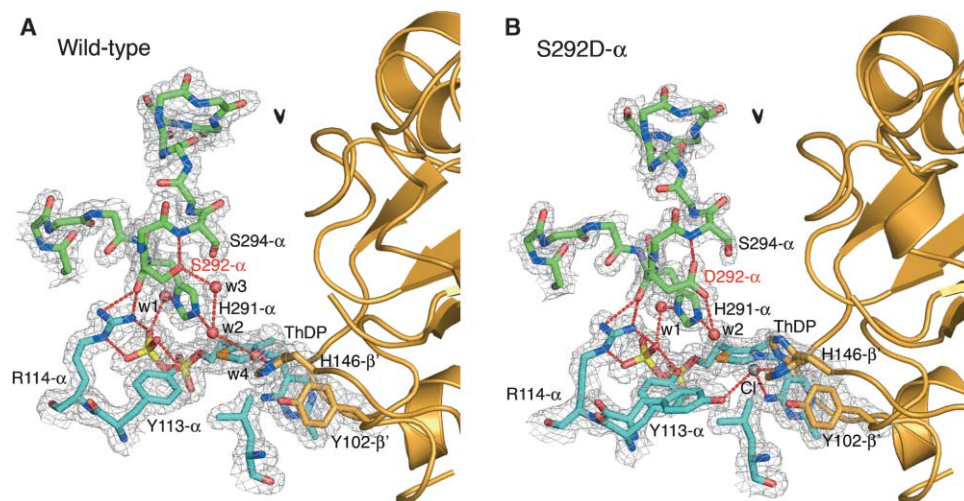


Figure 5. Electron Density Maps of the Phosphorylation Loops in Wild-Type and the S292D- α Mutant E1b Proteins

$2F_o - F_c$ electron densities are contoured at 1.0σ and overlaid onto the coordinates for the phosphorylation loop. Densities and coordinates represent the loop from the α subunit, whereas secondary structures from the β' subunit are indicated in bronze; side chains for H146- β' and Y102- β' are shown.

(A) Strong electron density is present for the Ser292- α (site 1) of the wild-type structure. Extensive hydrogen bonds exist in the wild-type structure, including the interaction between the side chain O γ atom of Ser292- α and the main chain amide group of Ser294- α (distance 3.0 Å). (B) The loop and hydrogen bonds in the wild-type structure are largely retained in the S292D- α structure. Strong electron density is also present for Asp292- α , which substitutes Ser292- α in maintaining interactions with Ser294- α (distance 2.8 Å). However, the water molecule (w4) in the wild-type structure is replaced by a nearby Cl $^-$ ion (silver sphere) in the S292D- α mutant structure. The side chain for Y113- α in the S292D- α structure represents two distinct conformations, as opposed to a single conformation in this wild-type structure. Two conformers are also present for the side chain of H146- β' in the S292D- α structure. Carbon atoms for the phosphorylation loop are shown in green, while nonloop residues are shown in cyan. ThDP is shown in cyan, the phosphorous atoms are shown in yellow, the sulfur atoms are shown in orange, the oxygen atoms are shown in red, and the nitrogen atoms are shown in blue. The arrow depicts an α -ketoacid substrate entering the active site channel. Graphics were generated with PyMol and were rendered within the PyMol program to produce the final figure.

channel to reach the bound cofactor ThDP. An extensive network of interactions mediated through water molecules (w1–w4) exists in the vicinity of Ser292- α (phosphorylation site 1). His291- α and Arg287- α interact with the phosphate oxygens of ThDP through the w1 molecule (Wynn et al., 2003). Figure 5A shows that the side chain O γ atom of Ser292- α is hydrogen bonded to the backbone amide of Ser294- α (within 3.0 Å distance) and the w3 water molecule. The elimination of these interactions in phosphorylated E1b or Ser292- α E1b mutants may impart a local (e.g., the S292N- α mutant) or overall (e.g., S292E- α and S292Q- α) disruption of the phosphorylation loop. It should also be pointed out that the side chain of Arg114- α forms hydrogen bonds to phosphate oxygen atoms of ThDP and the main chain carbonyl group of His291- α .

Based on the recently published structure of *Thermus thermophilus* E1b (Nakai et al., 2004), the carboxylate carbonyl group of substrate α -ketoisocaproate forms hydrogen bonds to side chains of Ser292- α and Gln98- β' through bridging water molecules, buttressed by an additional interaction with the N $^{\epsilon 2}$ atom of His291- α through the w2 water molecule in the human E1b structure (Figure 5A). The involvement of Ser292- α in stabilizing the bound α -ketoacid substrate is a structural basis for the markedly increased K_m for KIV of phosphorylated and mutant human E1b proteins (Tables 1 and 2). The substitution of Ser292- α with an alanine was previously shown to also increase the K_m for KIV by 10-fold over the wild-

type, as measured by the overall activity of the rat BCKDC (Zhao et al., 1994). This was supported in the present study by an over 20-fold higher K_m for KIV in the S292A- α mutant than the wild-type, according to E1b-catalyzed decarboxylation assayed in the presence of DCPIP (data not shown).

The substitution of Ser292- α with a small, negatively charged aspartic acid retains the local phosphorylation loop conformation through coordination of the aspartate side chain O $^{\delta 1}$ to the main chain amide of Ser294- α (2.8 Å) and O $^{\delta 2}$ to the w2 water molecule, with other hydrogen bonds largely remaining intact (Figure 5B). Therefore, the phosphorylation loop and the active site channel conformations are fully maintained with clear electron density in the S292D- α E1b structure. There are notable structural differences in the S292D- α mutant compared to the wild-type E1b, however, as it appears that the w4 water molecule in the wild-type is replaced by a Cl $^-$ ion (from the crystallization solution). At 1.72 Å resolution, one expects to see densities for water molecules if they are present in the vicinity of the Cl $^-$ ion in the S292D- α mutant. The side chain of His146- β' in the S292D- α variant adopts at least two distinguishable conformers through a rotation around the χ_1 torsion angle (between C $_{\alpha}$ and C $_{\beta}$) by about 90°. The His146- β' -conformer that coordinates to the Cl $^-$ ion is equivalent to the single conformation in the wild-type, which interacts with the w4 water molecule. Since His146- β' is near the putative substrate binding site (Evarsson et al., 1999),

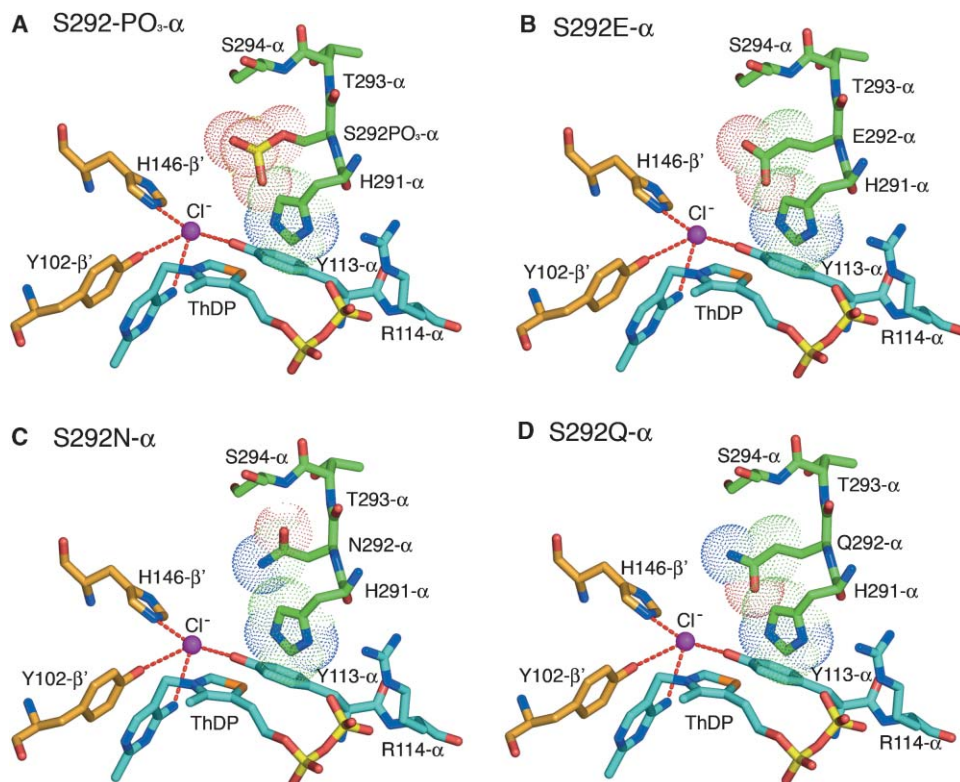


Figure 6. Predicted Steric Clashes in Phosphorylated, S292E- α , and S292Q- α E1b Structures

(A–D) In the (A) phosphorylated, (B) S292E- α , (C) S292N- α , and (D) S292Q- α structures, modeled van der Waals surfaces for the phosphoryl group or substituted residues, which predict steric clashes with His291- α , except Asn292- α , are based on coordinates of the wild-type structure in Figure 5A. These steric clashes result in the destabilization of the hydrogen bond network and therefore disorder the loop. Conformations for ThDP, Arg114- α , and the Cl⁻ ion that coordinates to the 4' amino group on the aminopyrimidine ring of ThDP, His146- β ' , and Tyr113- α are derived from $2F_o - F_c$ electron densities.

the dual conformers associated with this residue could, in part, account for the highest K_m for KIV of the S292D- α E1b among the mutants studied (Tables 1 and 2). In the ordered loop conformation, Asp292- α in the S292D- α variant protrudes into the active site channel and is juxtaposed above the thiazolium ring of the bound ThDP. The electrostatic repulsion posed by the aspartate residue in the active site channel is likely to also contribute to the reduced affinity of the S292D- α mutant for the substrate ketoacid. The negative charge of the aspartate residue may further interfere with the passage of lip-LBD with the electrophilic dithiolane ring through the active site channel, which could explain the weak interaction of the S292D- α mutant E1b with lip-LBD as indicated by ITC measurements. The Tyr113- α side chain in the S292D- α mutant also assumes two different positions, with one coordinating to the phosphate oxygen of ThDP, similar to the wild-type, and the other interacting with the Cl⁻ ion. The coordination of one of Tyr113- α 's side chains to the phosphate oxygen of ThDP is consistent with the ordered conformation of the phosphorylation loop in the S292D- α variant.

Steric Clashes between the Phosphoryl Group and His291- α Triggers the Disordering of the Loop

The incorporation of a phosphoryl group into the Ser292- α side chain results in disordering of the entire

phosphorylation loop (Figure 6A), whereas the region involving residues Tyr113- α , Arg114- α , Tyr102- β ' , and His146- β ' remains ordered. However, the stabilizing interaction between the Ser292- α O γ atom and the backbone amide of Ser294- α in the wild-type is lost. The entire water molecule-mediated hydrogen bond network is also absent in the phosphorylated E1b structure. The w4 molecule in wild-type E1b is replaced in phosphorylated E1b by a Cl⁻ ion, which coordinates to the side chain of His146- β ' , similar to what occurs in the S292D- α structure. The side chain of Tyr113- α in phosphorylated E1b, unlike S292D- α , now solely coordinates to the Cl⁻ ion and correlates with the disordered loop conformation. When modeled into the wild-type structure, the phosphoryl group of phosphorylated Ser292- α would clash with the side chain of His291- α (Figure 6A). Since His291- α is an indispensable anchor for ThDP (Figure 5A) (Wynn et al., 2003), steric effects on the side chain of His291- α could result in the overall disruption of the phosphorylation loop in phosphorylated E1b, similar to that observed with the H291A- α E1b variant (Wynn et al., 2003). The disordered loop prevents phosphorylated E1b from binding the E2b lipoyl-bearing domain, which effectively shuts off the E1b-catalyzed reductive acylation reaction and completely inactivates BCKDC. Since the loop is disordered in phosphorylated E1b (Figure 6A), the negative charges of the phosphoryl Ser292- α

Table 4. Statistical Data for Wild-Type, Phosphorylated, and Mutant E1b

	Wild-Type	S292D- α	S292Q- α	S292E- α	S292N- α	S292- α -PO ₃
Data Collection						
Unit cell (Å)	P3,21	P3,21	P3,21	P3,21	P3,21	P3,21
<i>a</i> = <i>b</i>	143.32	145.31	145.67	145.68	145.67	144.40
<i>c</i>	69.29	69.32	69.19	69.25	69.24	69.01
Wavelength (Å)	1.0	1.0	1.0	1.0	1.0	1.0
Resolution (Å)	1.83	1.72	1.73	2.10	1.57	2.00
Measurements	393,457	529,588	443,569	218,173	655,557	285,231
Unique reflections	71,894	89,234	86,997	48,283	117,257	53,838
Completeness (last shell) (%)	99.7 (100)	99.9 (98.8)	98.9 (98.0)	97.5 (71.8)	99.7 (96.1)	96.2 (76.0)
R _{merge} (last shell) (%)	10.6 (88.9)	6.2 (64.1)	6.8 (66.7)	9.5 (38.6)	5.1 (45.6)	7.4 (37.8)
I/ σ (last shell)	16.9 (2.1)	27.2 (1.9)	25.2 (1.9)	14.3 (2.1)	32.9 (2.0)	19.4 (2.3)
Refinement						
Number of reflections (work/test)	70,373/1,493	87,692/1,514	85,526/1,469	46,720/1,542	115,678/1,515	52,347/1,479
Number of atoms						
Protein	5,878	5,889	5,638	5,569	5,666	5,558
Solvents	487	656	622	489	744	398
Ions	3	4	4	4	4	4
Ligands	2	2	2	2	2	2
R _{work} (last shell) (%)	15.6 (21.7)	15.3 (24.5)	14.7 (25.7)	14.7 (20.1)	14.9 (21.0)	16.0 (21.8)
R _{free} (last shell) (%)	19.4 (29.8)	18.9 (29.0)	18.1 (32.1)	19.0 (23.4)	16.6 (23.8)	19.3 (25.6)
Rmsd						
Bond length (Å)	0.020	0.020	0.020	0.019	0.019	0.020
Bond angle (°)	1.659	1.598	1.697	1.622	1.748	1.744
Mean B value (Å ²)						
Protein	24.3	11.9	19.9	22.9	9.23	33.9
Solvents	33.1	33.1	34.3	31.3	35.3	41.3
ThDP	17.7	2.7	9.62	14.6	2.17	21.5
Coordinate error (Å)	0.077	0.061	0.059	0.097	0.045	0.111
Number of alternative conformations	21	23	15	7	18	6
Missing residues	1-5 α ; 302-305 α ; 1-13 β	1-5 α ; 303-305 α ; 1-13 β	1-6 α ; 288-312 α ; 1-13 β	1-6 α ; 288-312 α ; 1-13 β	1-6 α ; 288-312 α ; 1-13 β	1-6 α ; 288-312 α ; 1-13 β

side chain, unlike its counterpart in *E. coli* isocitrate dehydrogenase (Hurley et al., 1990), has little, if any, effect on the accessibility of substrate ketoacids to the active site channel.

The introduction of a large, negatively charged glutamate residue into position 292- α also results in a complete disordering of the phosphorylation loop through steric clashes with the His291- α residue (Figure 6B). The remaining active site conformations, including the Cl⁻ ion coordinations, resemble that observed with phosphorylated E1b. The structural data explain the complete inactivation of the rat BCKDC (Zhao et al., 1994) and human PDC (Korotchikina and Patel, 2001), when a glutamate residue replaces the site 1 serine.

Glutamine Substitution Mimics the Phosphoryl Group in Disrupting the Phosphorylation Loop

The steric effect of phosphoryl Ser292- α was further studied by substitutions with the uncharged residues asparagine and glutamine. The phosphorylation loop is disordered in the S292N- α mutant, with other regions of the active site present in ordered conformations (Figure 6C), similar to that seen in the phosphorylated E1b structure. The modeled van der Waals surface shows that Asn292- α would necessitate only minor structural changes in order to avoid steric interference with His291- α . The absence of the interaction between the Ser292- α O γ atom and the w3 water molecule (Figure

5A) in the S292N- α mutant may promote the release of water molecules that mediate the hydrogen bond network, and this release may lead to disruption of the local conformation and displacement of the phosphorylation loop. The hydrogen bond between the side chain O δ^1 atom of Asn292- α and the main chain amide of Ser294- α is preserved (data not shown). The fact that the phosphorylation loop conformation is only minimally disturbed in the S292N- α mutant is consistent with its near wild-type overall BCKDC activity.

The size effect of the phosphoryl group on the phosphorylation loop conformation as well as catalysis is readily reproduced in the S292Q- α mutant (Figure 6D). In this mutant E1b, glutamine in place of Ser292- α would result in structural rearrangements in order to avoid steric clashes with His291- α , similar to the effects of the phosphoryl group in phosphorylated E1b (Figure 6A). This could explain the disordering of the loop in this variant accompanied by the abrogation of reductive acylation and overall activity, similar to phosphorylated E1b (Figure 2). The only difference is the complete absence of decarboxylation activity (Reaction 2) in the S292Q- α mutant as opposed to the reduced corresponding activity in phosphorylated E1b. Since the phosphorylation loop is not ordered in both S292Q- α and phosphorylated E1b, more detailed structural insights cannot be provided to explain the difference in E1b-catalyzed decarboxylation activity between these

two E1b proteins. These results, taken together, establish that the size of the phosphoryl group alone is sufficient to account for the overall disruption of the phosphorylation loop, and this disruption results in the loss of E1b-mediated reductive acylation (Reaction 3) and the accompanying complete abolishment of BCKDC activity.

Experimental Procedures

Production of Wild-type E1b and Ser292- α Mutants

N-terminally His₆-tagged wild-type E1b and Ser292- α mutants were produced as described previously (Wynn et al., 2000). Forward primers for producing Ser292- α E1b mutants (with nucleotides changed from the wild-type sequence underlined) were as follows: 5'-CCTACAGGATCGGGCACCACGACACCAGTGACGACAGTTC-3' (S292D), 5'-CCTACAGGATCGGGCACCACGAGACCAGTGACGACAGTTC-3' (S292E), 5'-CCTACAGGATCGGGCACCACACACCAGTGACGACAGTTC-3' (S292N), and 5'-CCTACAGGATCGGGCACCACGACACCA GTGACGACAGTTC-3' (S292Q). The reverse primer for each mutant is of the complementary sequence to its respective forward primer. C-terminally His₆-tagged LBD (residues 1–84 of the E2b subunit) was expressed (Chuang et al., 2002) and lipoylated *in vitro* with D, L-thioctic acid (oxidized) by using LplA ligase as described previously (Chuang et al., 2000).

Phosphorylation of the S302A- α E1b Mutant

The phosphorylation reaction mixture contained 50 mM potassium phosphate (pH 7.5), 100 mM KCl, 5 mM Mg-ATP, 1 mM benzamidine, as well as the maltose binding protein-tagged rat BCKD kinase, S302A- α mutant E1b, and lipoylated E2b at the molar ratio of 2:12.5:3.3 or concentrations of 0.64, 2.27, or 3.63 mg/ml, respectively. After incubation at 30°C for 8 hr, NaCl was added to the mixture to a final concentration of 1 M. The mixture was further incubated for 30 min to allow for the complete dissociation of E1b from E2b and the kinase. Phosphorylated E1b was purified from dissociated E2b and the kinase on Ni-NTA and FPLC HiLoad Superdex 200 columns in 50 mM potassium phosphate (pH 7.5), 1 M NaCl, 5% (v/v) glycerol, and 5 mM dithiothreitol.

Binding Studies by Isothermal Titration Calorimetry

Human E1b and lip-LBD, both C-terminally His₆ tagged, were dialyzed exhaustively against the same buffer, and binding measurements were carried out by isothermal titration calorimetry as described previously, except a molar ratio of E1b heterotetramer: lip-LBD monomer was used (Wynn et al., 2003).

Enzyme Assays

The BCKDC was reconstituted with wild-type E1b or a Ser292- α mutant, lipoylated E2b, and E3 at a molar ratio of 12:1:55. The overall activity (Reaction 1) of the reconstituted BCKDC was assayed spectrophotometrically as described previously (Chuang et al., 2000). The E1b-catalyzed decarboxylation of KIV (Reaction 2) was also assayed spectrophotometrically in the presence of the artificial electron acceptor 2,6-dichlorophenolindophenol (DCPIP) as described previously (Chuang et al., 2004; Li et al., 2004). The E1b-catalyzed reductive acylation of lip-LBD was assayed with [¹⁴C]KIV and lip-LBD as substrates. Incorporation of the radiolabel into lip-LBD was determined as also described previously (Wynn et al., 2003).

ThDP Binding Measurements by Tryptophan Fluorescence Quenching

Steady-state tryptophan fluorescence quenching upon ThDP binding to wild-type and mutant E1b (Nemeria et al., 2001) was measured as described previously (Wynn et al., 2003). Fluorescence was corrected for the inner-filter effect at high ThDP concentrations (Lakowicz et al., 1983).

Crystallization of Wild-Type and Mutant E1b Proteins

The C-terminally His₆-tagged SBD protein was produced as described previously (Chuang et al., 2004). The E1b-SBD complex was formed by mixing N-terminally His₆-tagged wild-type E1b or Ser292- α

mutants with C-terminally His₆-tagged SBD at a molar ratio of 1:4. The mixture was concentrated in an Amicon Ultra concentrator (Millipore) to 20 mg/ml in 50 mM Na-HEPES (pH 7.5), 150 mM KCl, 20 mM DTT, and 5% (v/v) glycerol. Crystals of the E1b-SBD complex were obtained by the hanging-drop vapor diffusion technique at 20°C by mixing 3 μ l protein with 3 μ l crystallization solution (10% [w/v] polyethylene glycol 4000, 10% [v/v] 2-methyl-2, 4-pentandiol, and 0.1 M sodium citrate [pH 5.8]) with 0.75 ml crystallization solution in the reservoir. Crystals appeared in 1 day and grew to a maximum size of 200 \times 1600 μ m (with the former representing the diagonal dimensions of the hexagonal face) within 10 days. Crystals were stabilized for 12 hr by soaking in fresh crystallization solution containing 10 mM Mn-ThDP. Mn²⁺ ions were used to replace the Mg²⁺ required for the binding of ThDP to E1b (Wynn et al., 2003). Crystals were cryo-protected by transfer to the crystallization solution containing 10% (v/v) glycerol. Crystals were flash-cooled in liquid propane and kept at about 100K during data collection for the human E1b-SBD complex at beam lines 19ID and 19BM at the Advanced Photon Source, Argonne National Laboratory, Argonne, IL. Data sets were processed with the HKL2000 package (Otwinowski and Minor, 1997). Crystals obtained with this procedure exhibited the symmetry of space group P3₁21, with cell parameters of approximately 145 \times 145 \times 69 Å, and contained one $\alpha\beta$ heterodimer and half of an SBD molecule per asymmetric unit. The heterotetrameric molecule of E1b was generated by crystallographic symmetry. In the absence of substrate, there is no structural heterogeneity in the heterodimer that contains one of the two active sites of the E1b heterotetramer. They diffracted X-rays to a minimum Bragg spacing (d_{\min}) of 1.57 Å. The structure of E1b was solved and refined with the program Refmac5 from the CCP4 package (CCP4, 1994). The complete refinement statistics are shown in Table 4.

Acknowledgments

We thank Clint Moss for valuable technical assistance in this study. This work was supported by Grants DK-26758 and DK-62306 from the National Institutes of Health and Grant I-1286 from the Welch Foundation. Use of the Argonne National Laboratory Structural Biology Center beamlines at the Advanced Photon Source was supported by the U.S. Department of Energy, Office of Energy Research, under Contract No. W-31-109-ENG-38.

Received: July 28, 2004

Revised: September 13, 2004

Accepted: September 24, 2004

Published: December 7, 2004

References

- Ævarsson, A., Seger, K., Turley, S., Sokatch, J.R., and Hol, W.G. (1999). Crystal structure of 2-oxoisovalerate and dehydrogenase and the architecture of 2-oxo acid dehydrogenase multienzyme complexes. *Nat. Struct. Biol.* 6, 785–792.
- Ævarsson, A., Chuang, J.L., Wynn, R.M., Turley, S., Chuang, D.T., and Hol, W.G. (2000). Crystal structure of human branched-chain α -ketoacid dehydrogenase and the molecular basis of multienzyme complex deficiency in maple syrup urine disease. *Struct. Fold. Des.* 8, 277–291.
- Bilwes, A.M., Quezada, C.M., Croal, L.R., Crane, B.R., and Simon, M.I. (2001). Nucleotide binding by the histidine kinase CheA. *Nat. Struct. Biol.* 4, 353–360.
- Chauhan, H.J., Domingo, G.J., Jung, H.-I., and Perham, R.N. (2000). Sites of limited proteolysis in the pyruvate decarboxylase component of the pyruvate dehydrogenase multienzyme complex of *Bacillus stearothermophilus* and their role in catalysis. *Eur. J. Biochem.* 267, 7158–7169.
- CCP4 (Collaborative Computational Project, Number 4) (1994). The CCP4 suite: programs for protein crystallography. *Acta Crystallogr. D Biol. Crystallogr.* 50, 760–763.
- Chuang, D.T., and Shih, V.E. (2001). Maple syrup urine disease (branched-chain ketoaciduria). In *The Metabolic and Molecular Basis of Inherited Disease*, Eighth Edition, C.R. Scriver, A.L. Beaudet,

- W.S. Sly, D. Valle, B. Vogelstein, and B. Childs, eds. (New York, NY: McGraw-Hill), pp. 1971–2006.
- Chuang, J.L., Davie, J.R., Wynn, R.M., and Chuang, D.T. (2000). Production of recombinant mammalian holo-E2 and E3 and reconstitution of functional branched-chain α -keto acid dehydrogenase complex with recombinant E1. *Methods Enzymol.* 324, 192–200.
- Chuang, J.L., Wynn, R.M., and Chuang, D.T. (2002). The C-terminal hinge region of lipoic acid-bearing domain of E2b is essential for domain interaction with branched-chain α -keto acid dehydrogenase kinase. *J. Biol. Chem.* 277, 36905–36908.
- Chuang, J.L., Wynn, R.M., Moss, C.C., Song, J.L., Li, J., Awad, N., Mandel, H., and Chuang, D.T. (2004). Structural and biochemical basis for novel mutations in homozygous Israeli maple syrup urine disease patients: a proposed mechanism for the thiamin-responsive phenotype. *J. Biol. Chem.* 279, 17792–17800.
- Ciszak, E.M., Korotchkina, L.G., Dominiak, P.M., Sidhu, S., and Patel, M.S. (2003). Structural basis for flip-flop action of thiamin pyrophosphate-dependent enzymes revealed by human pyruvate dehydrogenase. *J. Biol. Chem.* 278, 21240–21246.
- Cook, K.G., Bradford, A.P., Yeaman, S.J., Aitken, A., Fearnley, I.M., and Walker, J.E. (1984). Regulation of bovine kidney branched-chain 2-oxoacid dehydrogenase complex by reversible phosphorylation. *Eur. J. Biochem.* 145, 587–591.
- Damuni, Z., and Reed, L.J. (1987). Purification and properties of the catalytic subunit of the branched-chain α -keto acid dehydrogenase phosphatase from bovine kidney mitochondria. *J. Biol. Chem.* 262, 5129–5132.
- Davie, J.R., Wynn, R.M., Meng, M., Huang, Y.-S., Aalund, G., Chuang, D.T., and Lau, K.S. (1995). Expression and characterization of branched-chain α -ketoacid dehydrogenase kinase from the rat: is it a histidine-protein kinase? *J. Biol. Chem.* 270, 19861–19867.
- Fries, M., Jung, H.I., and Perham, R.N. (2003). Reaction mechanism of the heterotetrameric (α 2 β 2) E1 component of 2-oxo acid dehydrogenase multienzyme complexes. *Biochemistry* 42, 6996–7002.
- Gaudet, R., Savage, J.R., McLaughlin, J.N., Willardson, B.M., and Sigler, P.B. (1999). A molecular mechanism for the phosphorylation-dependent regulation of heterotrimeric G proteins by phosducin. *Mol. Cell* 3, 649–660.
- Harris, R.A., Paxton, R., Goodwin, G.W., and Powell, S.M. (1986). Regulation of the branched-chain 2-oxo acid dehydrogenase complex in hepatocytes isolated from rats fed on a low-protein diet. *Biochem. J.* 234, 285–294.
- Harris, R.A., Hawes, J.W., Popov, K.M., Zhao, Y., Shimomura, Y., Sato, J., Jaskiewicz, J., and Hurley, T.D. (1997). Studies on the regulation of the mitochondrial α -ketoacid dehydrogenase complexes and their kinases. *Adv. Enzyme Regul.* 37, 271–293.
- Huang, Y.S., and Chuang, D.T. (1999). Down-regulation of rat mitochondrial branched-chain 2-oxoacid dehydrogenase kinase gene expression by glucocorticoids. *Biochem. J.* 339, 503–510.
- Hurley, J.H., Dean, A.M., Sohl, J.L., Koshland, D.E., Jr., and Stroud, R.M. (1990). Regulation of an enzyme by phosphorylation at the active site. *Science* 249, 1012–1016.
- Johnson, L.N., and Lewis, R.J. (2001). Structural basis for control by phosphorylation. *Chem. Rev.* 101, 2209–2242.
- Korotchkina, L.G., and Patel, M.S. (2001). Probing the mechanism of inactivation of human pyruvate dehydrogenase by phosphorylation of three sites. *J. Biol. Chem.* 276, 5731–5738.
- Krebs, E.G., Kent, A.B., and Fischer, E.H. (1958). The muscle phosphorylase b kinase reaction. *J. Biol. Chem.* 231, 73–83.
- Lakowicz, J.R.M., Cherek, B.P., and Ralter, A. (1983). Rotational freedom of tryptophan residues in proteins and peptides. *Biochemistry* 22, 1741–1752.
- Lander, E.S., Linton, L.M., Birren, B., Nusbaum, C., Zody, M.C., Baldwin, J., Devon, K., Dewar, K., Doyle, M., FitzHugh, W., et al. (2001). Initial sequencing and analysis of the human genome. *Nature* 409, 860–921.
- Li, J., Wynn, R.M., Machius, M., Chuang, J.L., Karthikeyan, S., Tomchick, D.R., and Chuang, D.T. (2004). Crosstalk between thiamin diphosphate binding and phosphorylation loop conformation in human branched-chain α -ketoacid decarboxylase/dehydrogenase. *J. Biol. Chem.* 279, 32968–32978.
- Linn, T.C., Pettit, F.H., and Reed, L.J. (1969). α -Keto acid dehydrogenase complexes. X. Regulation of the activity of the pyruvate dehydrogenase complex from beef kidney mitochondria by phosphorylation and dephosphorylation. *Proc. Natl. Acad. Sci. USA* 62, 234–241.
- Lu, G., Dobritsch, D., Baumann, S., Schnekider, G., and König, D. (2000). The structural basis of substrate activation in yeast pyruvate dehydrogenase. A crystallographic and kinetic study. *Eur. J. Biochem.* 267, 861–868.
- Machius, M., Chuang, J.L., Wynn, R.M., Tomchick, D.R., and Chuang, D.T. (2001). Structure of rat BCKD kinase: nucleotide-induced domain communication in a mitochondrial protein kinase. *Proc. Natl. Acad. Sci. USA* 98, 11218–11223.
- Majer, M., Popov, K.M., Harris, R.A., Bogardus, C., and Prochazka, M. (1998). Insulin downregulates pyruvate dehydrogenase kinase (PDK) mRNA: potential mechanism contributing to increased lipid oxidation in insulin-resistant subjects. *Mol. Genet. Metab.* 65, 181–186.
- Nakai, T., Nakagawa, N., Maoka, N., Masui, R., Kuramitsu, S., and Kamiya, N. (2004). Ligand-induced conformational changes and a reaction intermediate in branched-chain 2-oxo acid dehydrogenase (E1) from *Thermus thermophilus* HB8, as revealed by X-ray crystallography. *J. Mol. Biol.* 337, 1011–1033.
- Nemeria, N., Yan, Y., Zhang, Z., Brown, A.M., Arjunan, P., Furey, W., Guest, J.R., and Jordan, F. (2001). Inhibition of the *Escherichia coli* pyruvate dehydrogenase complex E1 subunit and its tyrosine 177 variants by thiamin 2-thiazolone and thiamin 2-thiothiazolone diphosphates. Evidence for reversible tight-binding inhibition. *J. Biol. Chem.* 276, 45969–45978.
- Otwinowski, Z., and Minor, W. (1997). Processing of X-ray diffraction data collected in oscillation mode. *Methods Enzymol.* 276, 307–326.
- Paul, H.S., and Adibi, S.A. (1982). Activation of hepatic branched chain α -keto acid dehydrogenase by a skeletal muscle factor. *J. Biol. Chem.* 257, 12581–12588.
- Perham, R.N. (2000). Swinging arms and swinging domains in multifunctional enzymes: catalytic machines for multistep reactions. *Annu. Rev. Biochem.* 69, 961–1004.
- Reed, L.J., Damuni, Z., and Merryfield, M.L. (1985). Regulation of mammalian pyruvate and branched-chain α -keto acid dehydrogenase complexes by phosphorylation dephosphorylation. *Curr. Top. Cell. Regul.* 27, 41–49.
- Robinson, B.L. (2001). Lactic acidemia: disorders of pyruvate carboxylase and pyruvate dehydrogenase. In *The Metabolic and Molecular Basis of Inherited Disease*, Eighth Edition, C.R. Scriver, A.L. Beaudet, W.S. Sly, D. Valle, B. Vogelstein, and B. Childs, eds. (New York, NY: McGraw-Hill), pp. 2275–2295.
- Sprang, S.R., Acharya, K.R., Goldsmith, E.J., Stuart, D.I., Varvill, K., Fletterick, R.J., Madsen, N.B., and Johnson, L.N. (1988). Structural changes in glycogen phosphorylase induced by phosphorylation. *Nature* 336, 215–221.
- Sugden, P.H., and Randle, P.J. (1978). Regulation of pig heart pyruvate dehydrogenase by phosphorylation. Studies on the subunit and phosphorylation stoichiometries. *Biochem. J.* 173, 659–668.
- Wynn, R.M., Davie, J.R., Song, J.L., Chuang, J.L., and Chuang, D.T. (2000). Expression of E1 component of human branched-chain α -keto acid dehydrogenase complex in *Escherichia coli* by cotransformation with chaperonins GroEL and GroES. *Methods Enzymol.* 324, 179–191.
- Wynn, R.M., Machius, M., Chuang, J.L., Li, J., Tomchick, D.R., and Chuang, D.T. (2003). Roles of His291- α and His146- β in the reductive acylation reaction catalyzed by human branched-chain alpha-ketoacid dehydrogenase: refined phosphorylation loop structure in the active site. *J. Biol. Chem.* 278, 43402–43410.
- Yeaman, S.J., Hutchenson, E.T., Roche, T.E., Pettit, F.H., Brown, J.R., Reed, L.J., Watson, D.C., and Dixon, G.H. (1978). Sites of phosphorylation on pyruvate dehydrogenase from bovine kidney and heart. *Biochemistry* 17, 2364–2370.

Zhao, Y., Denne, S.C., and Harris, R.A. (1993). Developmental pattern of branched-chain 2-oxo acid dehydrogenase complex in rat liver and heart. *Biochem. J.* 290, 395–399.

Zhao, Y., Hawes, J., Popov, K.M., Jaskiewicz, J., Shimomura, Y., Crabb, D.W., and Harris, R.A. (1994). Site-directed mutagenesis of phosphorylation sites of the branched chain alpha-ketoacid dehydrogenase complex. *J. Biol. Chem.* 269, 18583–18587.

Accession Numbers

The coordinates have been deposited in the Protein Data Bank (codes 1U5B, 1X7W, 1X7X, 1X7Y, 1X7Z, and 1X80).